METHODS & TECHNIQUES

Electroporation of adherent cells with low sample volumes on a microscope stage

Harunobu Tsugiyama[1], Chika Okimura[1], Takafumi Mizuno[2] and Yoshiaki Iwadate[1,3,*]

[1]Department of Functional Molecular Biology, Graduate School of Medicine, Yamaguchi University, Yamaguchi 753-8512, Japan,
[2]Biomedical Research Institute, National Institute of Advanced Industrial Science and Technology (AIST), Tsukuba 305-8566, Japan
and [3]PRESTO, Japan Science and Technology Agency, 4-1-8 Honcho Kawaguchi, Saitama 332-0012, Japan
*Author for correspondence (iwadate@yamaguchi-u.ac.jp)

SUMMARY

The labeling of specific molecules and their artificial control in living cells are powerful techniques for investigating intracellular molecular dynamics. To use these techniques, molecular compounds (hereinafter described simply as 'samples') need to be loaded into cells. Electroporation techniques are exploited to load membrane-impermeant samples into cells. Here, we developed a new electroporator with four special characteristics. (1) Electric pulses are applied to the adherent cells directly, without removing them from the substratum. (2) Samples can be loaded into the adherent cells while observing them on the stage of an inverted microscope. (3) Only 2 µl of sample solution is sufficient. (4) The device is very easy to use, as the cuvette, which is connected to the tip of a commercially available auto-pipette, is manipulated by hand. Using our device, we loaded a fluorescent probe of actin filaments, Alexa Fluor 546 phalloidin, into migrating keratocytes. The level of this probe in the cells could be easily adjusted by changing its concentration in the electroporation medium. Samples could be loaded into keratocytes, neutrophil-like HL-60 cells and *Dictyostelium* cells on a coverslip, and keratocytes on an elastic silicone substratum. The new device should be useful for a wide range of adherent cells and allow electroporation for cells on various types of the substrata.

Supplementary material available online at http://jeb.biologists.org/cgi/content/full/216/19/3591/DC1

INTRODUCTION

The labeling of specific molecules and their artificial control in living cells are powerful techniques for the investigation of intracellular molecular dynamics. To use these techniques, various substances such as fluorescent dyes, caged compounds and plasmid vectors are loaded into the cells.

The application of electric field pulses to cells induces transient permeabilization of the plasma membrane: this process is called electroporation (Chang and Reese, 1990; Kinosita and Tsong, 1977; Zimmermann et al., 1976). Electroporation techniques are employed to load membrane-impermeant molecular compounds into cells. For typical applications using a conventional commercially available electroporator, electric pulses are applied to a cuvette, typically several tens of microliters in volume, containing the cell suspension and the sample to be loaded into the cell. Thus, application of this type of electroporator requires the adherent cells to be removed from the substratum.

To avoid causing physiological damage by this process, several electroporation techniques have been developed in which electric pulses are applied to the adherent cells directly, without removing them from the substratum (Boitano et al., 1992; Raptis et al., 2008; Teruel and Meyer, 1997; Yang et al., 1995; Zheng and Chang, 1991). A technique using a special glass slide coated with transparent conductive indium–tin oxide (ITO) was developed by Raptis and co-workers (Raptis et al., 2008). As this device can be placed on the stage of an inverted microscope, cells loaded with a sample can be observed *via* the objective lens of the microscope. This is a great advantage, because a particular colony of cells to which the electric

pulses need to be applied can be selected. However, this technique requires an expensive specially coated slide and a large sample volume. Using a small amount of sample with no special tools has an important advantage in that it reduces the cost of experimentation. Teruel and Meyer (Teruel and Meyer, 1997) developed another device that requires a very small volume of sample, 0.5–2 µl, for electroporation of adherent cells, although the device could not be placed on a microscope stage.

We have developed a new electroporator that has both of the above favorable characteristics, i.e. it can be set on the microscope stage and requires a very small sample volume. Fish epidermal keratocytes are used as a model system for studying the mechanics of crawling cell migration (Lee et al., 1993). Here, we describe our new electroporator and give examples of its ease of use for loading a filamentous actin (F-actin) probe, Alexa Fluor phalloidin, into migrating keratocytes to investigate the relationship between cell migration and the actin cytoskeleton. Samples could be loaded into keratocytes, HL-60 cells and *Dictyostelium* cells on a coverslip, and keratocytes on an elastic silicone substratum. The new device should be useful for a wide range of adherent cells and allow electroporation for cells on various types of the substrata.

MATERIALS AND METHODS

The overall setup for the new electroporator is shown in Fig. 1A. The device is composed of a high-voltage source, a large capacitor, an electric circuit and an electroporation cuvette that is equipped with an auto-pipette tip.

A

Auto-pipette

Tip

Cuvette

High-voltage source

Large capacitor

Electric circuit

B

Electrodes

0.1 mm

C

5 mm

5 mm

D

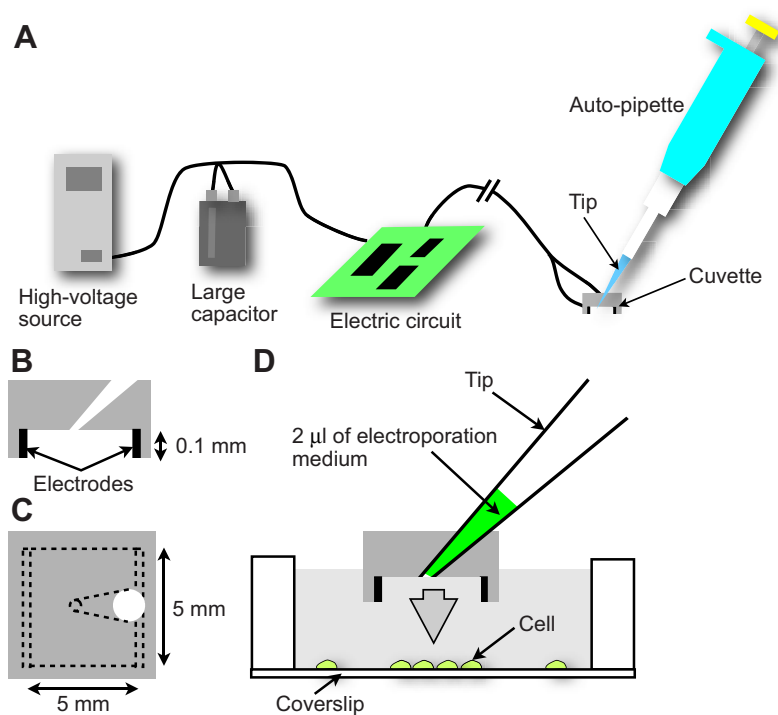Tip

2 μl of electroporation medium

Cell

Coverslip

Fig. 1. Diagram of the new electroporator. (A) Overall setup. The device is composed of a high-voltage source, a large capacitor (10,000 μF), an electric circuit and an electroporation cuvette equipped with a commercially available 10 μl short tip of an auto-pipette. (B,C) Cross-section and top view of the electroporation cuvette. The electroporation area is a 5×5×0.1 mm region with a pair of platinum sheet electrodes placed on two of its sides. There is a hole at the top of the cuvette, to which the tip of an auto-pipette is connected. (D) Application of the electroporator. The cuvette is attached to the coverslip to which cells are adhered by lowering the auto-pipette by hand. Immediately after discharge of electroporation medium (2 μl) into the space enclosed by the cuvette, electric field pulses are applied to the medium between the electrodes.

Preparation of electroporation cuvette

The electroporation cuvette (Fig. 1B,C) was made from an acrylic board using an NC milling machine (Cobra 2520; Original Mind, Nagano, Japan). The actual electroporated area is a 5×5×0.1 mm region with two platinum sheet electrodes placed on two of its sides. There is a hole at the top of the cuvette, to which a commercially available 10 μl short tip of an auto-pipette is connected.

Preparation of keratocytes on a coverslip

Primary cultures of fish epidermal keratocytes were prepared as described previously (Mizuno and Sekiguchi, 2011; Mizuno et al., 2003), with small modifications. Briefly, a goldfish, *Carassius auratus* (Linnaeus 1758), was anesthetized with Tricaine. Fish scales were extracted with tweezers and washed in culture medium – DMEM supplemented with 10% fetal calf serum and antibiotic/antimycotic solution (Sigma-Aldrich, St Louis, MO, USA). The scales were placed external side up on the bottom of a square chamber (18×18 mm and 2 mm in depth), the bottom of which was made of a 22×22 mm coverslip (No. 1, Matsunami, Osaka, Japan), then covered with another coverslip and allowed to adhere to the bottom coverslip for 1 h in 5% CO_2 at 37°C. Then, after removal of the upper coverslip, culture medium was added to the chamber and the scales were kept at 5% CO_2 and 37°C again overnight to allow the cells to spread from the scale and begin to migrate as single cells.

Preparation of keratocytes on an elastic substratum

Elastic sheets, 22 mm×40 mm×200 μm, were made from polydimethylsiloxane (Sylgard 184, Dow Corning Toray, Tokyo, Japan) according to the methods described previously (Iwadate and Yumura, 2009; Iwadate et al., 2013). Both 22 mm sides of the sheet were fixed. The surface of the sheet was coated with collagen (Cellmatrix I-C, Nitta Gelatin, Osaka, Japan). Keratocytes were prepared on the elastic sheet in the same manner as those on the coverslip.

Electroporation medium

A fluorescent dye, Oregon Green 488 BAPTA-1 dextran, potassium salt, 10,000 MW (O-6798; Life Technologies, Carlsbad, CA, USA), was dissolved in Ginzburg Fish Ringer's solution (GFR, mmol l^{-1}: 111.3 NaCl, 3.35 KCl, 2.7 $CaCl_2$ and 2.3 $NaHCO_3$, pH 7.6) including 0.5 mmol l^{-1} $MgSO_4$, resulting in a final concentration of 1 mmol l^{-1} Oregon Green. In this study, we used the dye as a large, 10,000 MW, load with a fluorescent tag rather than as a Ca^{2+} indicator. Alexa Fluor 546 phalloidin (A22283; Life Technologies) was dissolved in DMSO and then diluted 20 times with GFR containing 0.5 mmol l^{-1} $MgSO_4$, resulting in final concentrations of 100 μmol l^{-1} Alexa phalloidin and 5% DMSO.

Electroporation of keratocytes

The culture medium in the chamber was carefully replaced with Dulbecco's phosphate-buffered saline with Ca^{2+} and Mg^{2+} (PBS++). The tip of an auto-pipette, into which 2 μl of electroporation medium had been sucked beforehand, was inserted into the electroporation cuvette (Fig. 1D; supplementary material Movie 1). The auto-pipette was carefully lowered by hand until the bottom of the cuvette attached to the surface of the coverslip on which the cells had adhered (supplementary material Movie 2). Just after the discharge of the electroporation medium into the space (enclosed by the cuvette), electric field pulses were applied to the medium between the electrodes (Fig. 1B) using a simple self-made electric circuit (Fig. 2A–D).

Electric charge from a high-voltage source (MP-7812N, Oriental Instruments, Sagami, Japan) was stored in a large 10,000 μF capacitor (C in Fig. 2A) (EKMH251LGC103MEE0M, Nippon Chemi-Con, Tokyo, Japan). The charge was then applied to the medium between the electrodes, connected to E in Fig. 2A, through the photoMOS relay (AQV216, Panasonic, Tokyo, Japan) by pushing the switch of the electric circuit (SW$_0$ in Fig. 2A). The time of application was optimized using a one-shot multi-vibrator circuit (gray in Fig. 2A except AQV216) with an
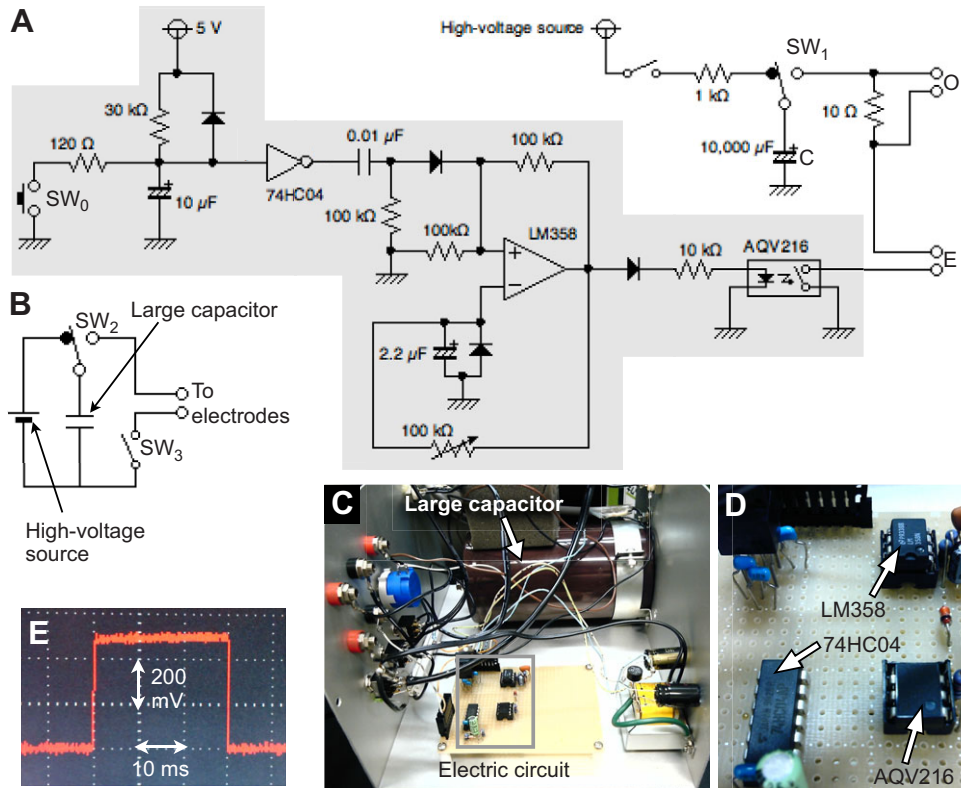
Fig. 2. (A) The electric circuit. Electrodes and a digital storage oscilloscope to monitor the waveform of electric pulses are connected to E and O, respectively. Electric charge from the high-voltage source is stored in the large (10,000 µF) capacitor (labeled C). The charge is applied to the medium between the electrodes through a photoMOS relay (AQV216) by pushing switch SW_0. The time of the application is optimized by a one-shot multi-vibrator circuit (gray, except AQV216) with an operational amplifier (LM358). (B) Simplified schematic diagram of A. Switches SW_2 and SW_3 are equivalent to SW_1 and the gray area in A, respectively. (C) Pictures of the real circuit. (D) Enlarged view of the area outlined in gray in C. (E) The waveform of the current across the electrodes was recorded via a 10 Ω resistor, using the digital storage oscilloscope connected to O in A.

operational amplifier, LM358 (Texas Instruments, Dallas, TX, USA). The current across the electrodes was measured via a 10 Ω resistor using a digital storage oscilloscope (PDS5022S, Owon, Xiamen, China), connected to O in Fig. 2A. To understand the complicated real circuit (Fig. 2A), a simplified schematic diagram and pictures of the real circuit are shown in Fig. 2B–D. Switches, SW_2 and SW_3, in Fig. 2B are equivalent to SW_1 and the gray area, respectively, in Fig. 2A. Fig. 2D is an enlarged view of the area outlined in gray in Fig. 2C.

The total time from the sucking up of electroporation medium to the application of electric pulses can be kept to less than 1 min. Just after the application of electric pulses, PBS++ was replaced with the culture medium for recovery of cells and subsequent observation. After about 5 min, cells were allowed to recover for observation.

Electroporation of HL-60 cells

Neutrophil-like HL-60 cell line, a model of human promyelocytic leukemia, was grown in RPMI 1640 medium supplemented with 10% FBS, 100 U ml^{-1} streptomycin and 100 U ml^{-1} penicillin G. To induce differentiation of the cells, they were transferred into culture medium containing 1.3% DMSO. After 4 days, cells showed neutrophil-like migration. The electroporation procedure for HL-60 cells was same as that for keratocytes.

Electroporation of *Dictyostelium* cells

Dictyostelium discoideum cells were cultured in HL5 medium [1.3% (w/v) bacteriological peptone, 0.75% (w/v) yeast extract, 85.5 mmol l^{-1} D-glucose, 3.5 mmol l^{-1} Na$_2$HPO$_4$, 3.5 mmol l^{-1} KH$_2$PO$_4$, pH 6.4] and developed until they became aggregation competent in BSS (10 mmol l^{-1} NaCl, 10 mmol l^{-1} KCl, 3 mmol l^{-1} CaCl$_2$) (Iwadate et al., 2013). The cell line used was AX2 cells (referred to as wild-type cells but actually an axenic derivative of

the wild-type strain NC4). In electroporation of *Dictyostelium* cells, BSS was used instead of the PBS++ and culture medium used for keratocytes. Electric charge was applied in the same manner as for keratocytes.

Microscopy

The migrating keratocytes loaded with fluorescent dye (Oregon Green or Alexa phalloidin) by electroporation were observed using an inverted microscope (Ti; Nikon, Tokyo, Japan) equipped with a laser confocal scanner unit (CSU-X1; Yokogawa, Tokyo, Japan) with a 100× objective lens (CFI Apo TIRF 100×H/1.49; Nikon, Tokyo, Japan). The fluorescence images were detected using an EM CCD camera (DU897; Andor, Belfast, UK).

Estimation of loading efficiency

Loading efficiency was estimated using the method of Teruel and Meyer (Teruel and Meyer, 1997) with slight modification. Briefly, the approximate loading efficiency of Oregon Green molecules into the cytosol was determined by comparing the confocal fluorescence intensity of Oregon Green in each cell with that of dilutions of the electroporation medium placed between two coverslips. The electroporation medium was diluted with a medium that included 10 mmol l^{-1} EDTA (pH 7.3, adjusted with NaOH). EDTA was used to chelate any free Ca^{2+} that might increase the fluorescence intensity of Oregon Green. For example, in the case when the fluorescence intensity of Oregon Green in a cell was same as that of a 0.2-fold diluted electroporation medium, the loading efficiency was determined to be 20% (Fig. 3D).

Estimation of rates of leading edge expansion and retrograde F-actin flow by fluorescence speckle microscopy

The use of our electroporation device allowed us to perform fluorescence speckle microscopy (FSM). To be able to compare the
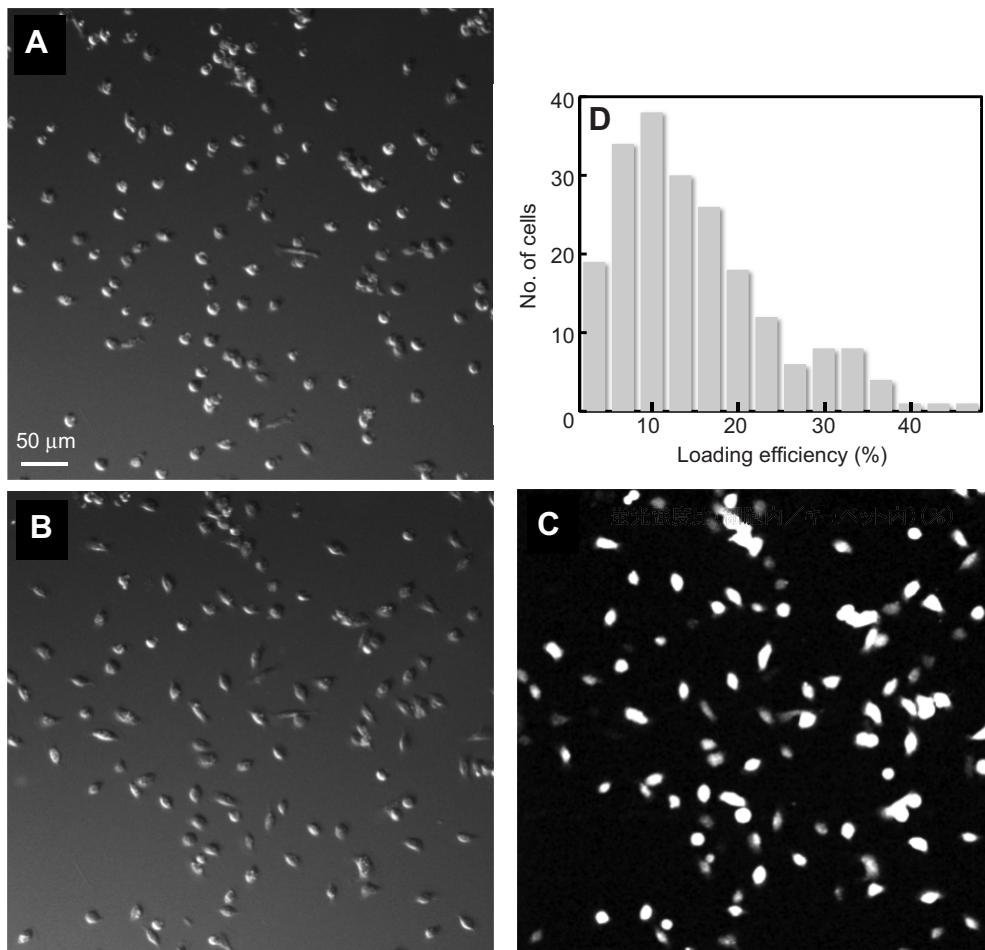
Fig. 3. Loading of Oregon Green into migrating keratocytes. Electric field pulses of $300\,V\,cm^{-1}$ amplitude and $30\,ms$ duration were applied to the medium between the electrodes twice, at an interval of $20\,s$. (A) Differential interference contrast (DIC) image of migrating keratocytes just after the replacement of culture medium with PBS++. The cells are slightly rounded because of replacement of the medium. (B) DIC image of electroporated cells $5\,min$ after application of the electric pulses. In response to the shock of the electric pulses, the cells returned to a fan-shaped morphology and began active crawling migration without detaching from the substratum. (C) Fluorescence image of the same cells as in B. (D) Histogram of the Oregon Green concentration in each cell, shown as a percentage of its concentration in the electroporation medium (i.e. loading efficiency).

rate of leading edge expansion and retrograde F-actin flow at the center with that at the sides of the lamellipodium, the 'center' and 'side' positions were defined as shown in Fig. 4F. First, a circle (the dashed line in Fig. 4F) was drawn by extending the arc line of the leading edge of a migrating keratocyte in a differential interference contrast (DIC) image of a particular time ($t=t_0$). A straight line (l_C in Fig. 4F) was drawn parallel to the migrating direction from the center (o in Fig. 4F) of the circle. Another straight line (l_S in Fig. 4F) was drawn $30\,deg$ from l_C, in a counter-clockwise direction. A $3\times5\,\mu m$ rectangle was then drawn ('Center' in Fig. 4F). The midpoint of the top side of the rectangle (c_0) was the intersection of l_C and the leading edge of the cell at $t=t_0$. A side rectangle ('Side' in Fig. 4F) and s_0 were drawn in the same manner as the center rectangle and c_0. In each rectangle, the average rate of bright dots of Alexa phalloidin was defined as that of retrograde F-actin flow there.

The intersections of l_C and the reading edge at $t=t_0+10\,s$ was defined as c_1. That of l_S and the reading edge at $t=t_0+10\,s$ was defined as s_1. The rate of leading edge expansion at the center at $t=t_0$ was defined as a value obtained by dividing the distance between c_0 and c_1 by $10\,s$. The rate of leading edge expansion at the side was defined in the same manner as for the center using s_0 and s_1.

RESULTS
Efficiency of electroporation using the new device

To confirm the usefulness of the new electroporator (Fig. 1) for loading membrane-impermeable substances into adherent cells, we first tried to load a fluorescent dye, Oregon Green dextran $10,000\,MW$, into migrating keratocytes.

Immediately after replacement of the culture medium in the chamber by PBS++, the chamber was placed on the stage of the inverted microscope. A colony of migrating cells was then set at the center of the visual field of the microscope by manipulating the stage. At this point, the cells became slightly rounded due to replacement of the medium (Fig. 3A). Electroporation was then performed using the procedure shown in Materials and methods. Electric field pulses of $300\,V\,cm^{-1}$ amplitude and $30\,ms$ duration were applied to the medium between the electrodes twice at an interval of $20\,s$. The pulse showed a clear square waveform without exponential decay (Fig. 2E).

Fig. 3B,C shows a DIC image and a fluorescence image of migrating keratocytes, $5\,min$ after application of the electric pulses. Most of the cells in Fig. 3B had a large expanded lamellipodium, which is typical of keratocytes, and actively migrated without detachment from the substratum as a result of the shock of the electric pulses (compare Fig. 3A and 3B). Fluorescence from Oregon Green was detected in 76 of 83 cells that had been subjected to the electric pulses (Fig. 3C). The loading efficiency of all cells from three experiments is summarized in Fig. 3D. The mode and mean of the histogram are 10% and 15%, respectively.

Staining of stress fibers with Alexa phalloidin in live keratocytes using the new electroporator

We planned to apply the new electroporator to study the cell migration of keratocytes. Electroporation medium that included $100\,\mu mol\,l^{-1}$ Alexa Fluor 546 phalloidin was prepared and electric field pulses were applied in the same manner as above. A typical
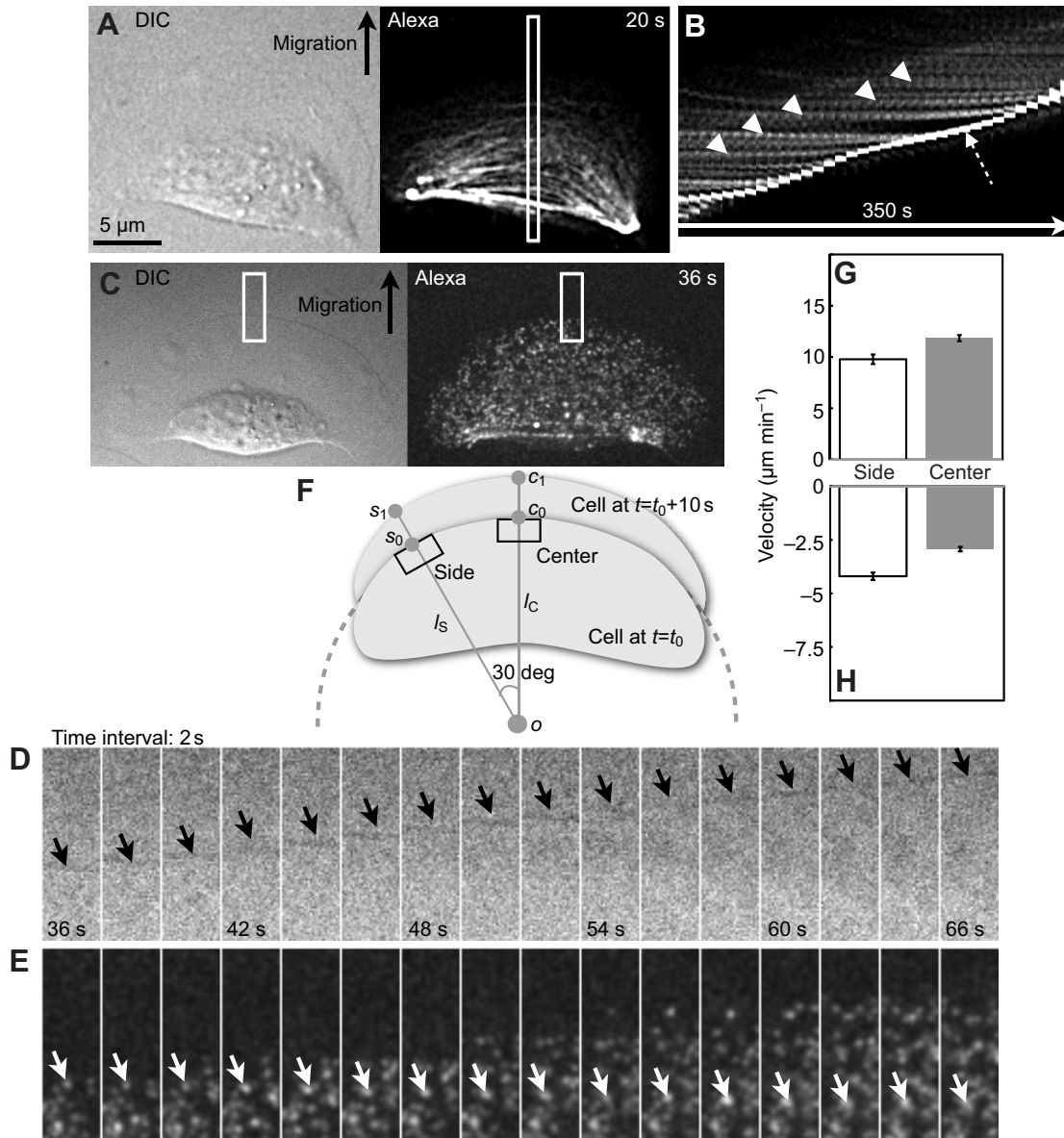
Fig. 4. Loading of Alexa Fluor 546 phalloidin into migrating keratocytes for observation of actin dynamics. (A,B) Observation of stress fibers in the cell body. A 2 µl sample of electroporation medium including 100 µmol l⁻¹ Alexa phalloidin was discharged into the space enclosed by the cuvette and the coverslip on which cells were adhered. Electric field pulses of 300 V cm⁻¹ amplitude and 30 ms duration were applied twice at an interval of 20 s. Thirty-five consecutive images were recorded every 10 s (supplementary material Movie 3). A DIC image and a fluorescence image at 20 s (A) were selected from the consecutive images. A kymograph (B) was constructed from image strips (white rectangle in A) taken from consecutive images. Arrowheads, stress fibers in the middle of the cell; dashed arrow, cell rear end including accumulated stress fibers. (C–H) Fluorescence speckle observation of retrograde F-actin flow in lamellipodium. A 2 µl sample of electroporation medium including 25 µmol l⁻¹ Alexa phalloidin was discharged into the space enclosed by the cuvette and a coverslip on which cells were adhered. Electric field pulses of 300 V cm⁻¹ amplitude and 30 ms duration were applied twice at an interval of 20 s. Forty-eight consecutive images were recorded every 2 s (supplementary material Movie 4). A DIC image and a fluorescence image at 36 s (C) were selected from the consecutive images. A region including the center of the leading edge (white rectangles in C) of the consecutive images is shown in D and E. The leading edge moved ahead (black arrows in D), while the bright spots showed retrograde movement (white arrows in E). The center and the side areas in the lamellipodium were defined as two rectangles ('Center' and 'Side' in F), with length 3 µm and width 5 µm (see Materials and methods for details). Rates of leading edge expansion ($N=9$) and retrograde F-actin flow ($N=9$) are shown in G and H, respectively (means ± s.e.m.). The rate of leading edge expansion at the center area was faster than that at the sides ($P=0.002$, t-test), whereas the rate of retrograde F-actin flow showed the opposite pattern ($P=1\times10^{-5}$, t-test).

cell subjected to electric pulses is shown in Fig. 4A and supplementary material Movie 3. The focus was kept at a height of 1.5 µm from the bottom of the cell body throughout the recording. Stress fibers are seen connecting the left and right ends of the cell (right-hand image in Fig. 4A). The dynamics of the stress fibers were estimated by constructing a kymograph (Fig. 4B) from

thin image strips (white rectangle in Fig. 4A) taken from 35 consecutive images. In the kymograph, white lines (arrowheads in Fig. 4B) reflecting the movement in the longitudinal direction of the stress fibers are aligned horizontally, indicating that the stress fibers do not move with respect to the lab frame of reference during cell migration. The bright slope (dashed arrow in Fig. 4B) is the
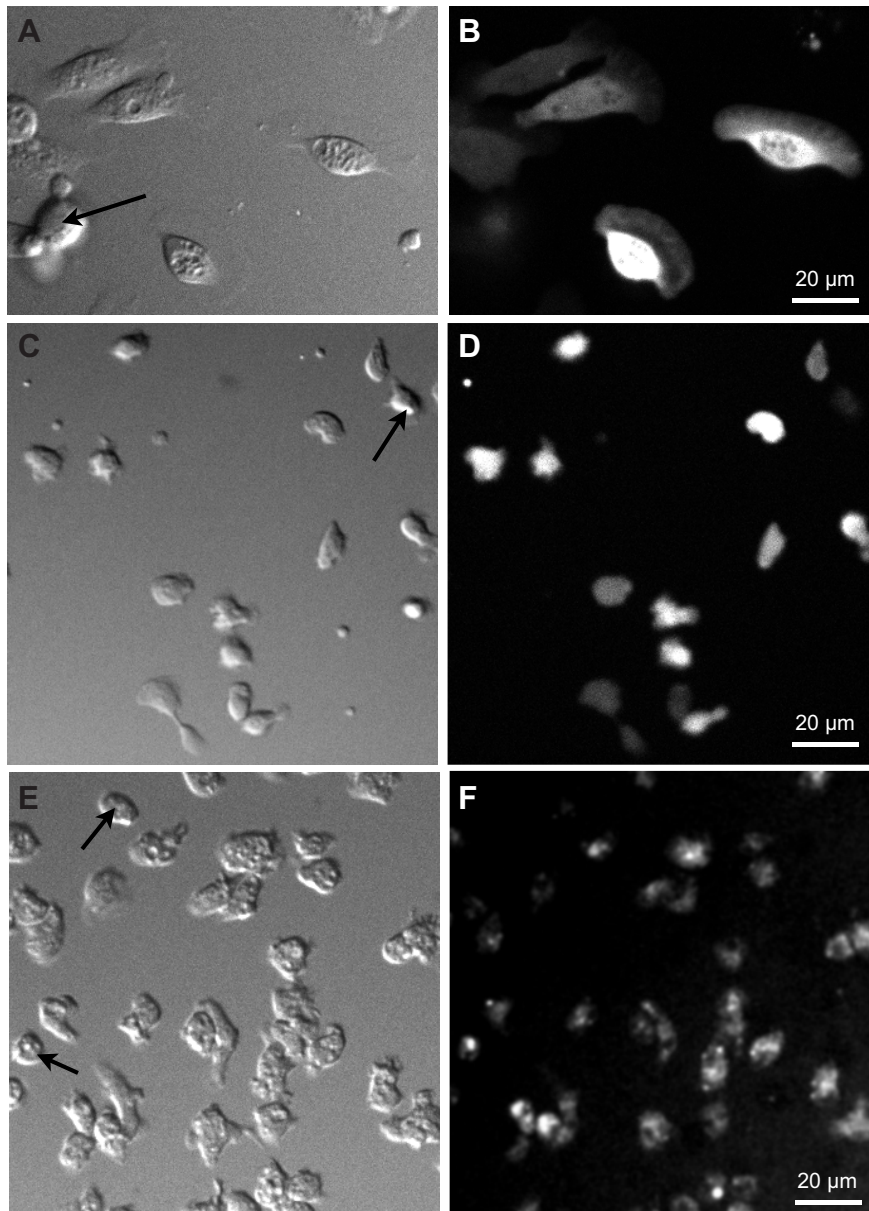
Fig. 5. Loading of Oregon Green into migrating keratocytes on an elastic substratum, and HL-60 cells and *Dictyostelium* cells on a coverslip. (A) DIC image of typical electroporated keratocytes on an elastic substratum 5 min after application of an electric pulse. Electric field pulses of 300 V cm^{-1} amplitude and 30 ms duration were applied to PBS++ between the electrodes twice, at an interval of 20 s. (B) Fluorescence image of the same cells as in A. (C) DIC image of electroporated HL-60 cells on a coverslip 5 min after application of an electric pulse. Electric field pulses of 400 V cm^{-1} amplitude and 30 ms duration were applied to PBS++ between the electrodes twice, at an interval of 20 s. (D) Fluorescence image of the same cells as in C. (E) DIC image of electroporated *Dictyostelium* cells on a coverslip 5 min after application of an electric pulse. Electric field pulses of 300 V cm^{-1} amplitude and 30 ms duration were applied to BSS between the electrodes twice, at an interval of 20 s. (F) Fluorescence image of the same cells as in E. Only a few cells were rounded as a result of the shock of the electric pulses (black arrows).

cell rear edge including accumulated stress fibers. The accumulated fibers moved forward as the cell advanced.

Speckle staining of F-actin with Alexa phalloidin in live keratocytes using the new electroporator

To visualize speckle staining of F-actin to estimate the rate of retrograde F-actin flow, Alexa phalloidin was adjusted to a concentration of 25 µmol l^{-1} by diluting the electroporation medium with the GFR, including 0.5 mmol l^{-1} MgSO$_4$, and electric field pulses were applied in the same manner as above. A typical cell subjected to the electric pulses is shown in Fig. 4C and supplementary material Movie 4. The focus was kept at the bottom of the lamellipodium throughout the recording. Many small bright dots are clearly seen throughout the cell (right image of Fig. 4C). From the sequential images, small regions including the center of the leading edge (the white rectangles in Fig. 4C) were cropped and aligned sequentially (Fig. 4D,E). The leading edge moved forward (Fig. 4D), while the dots showed retrograde movement (Fig. 4E), indicating that the movement of the dots tracked the retrograde F-

actin flow. If keratocytes migrate in accordance with the graded radial extension (GRE) model (Grimm et al., 2003; Lee et al., 1993; Mizuno et al., 1996; Mogilner and Keren, 2009), expansion of the leading edge at the center should be faster than that at the sides, whereas retrograde F-actin flow at the center should be slower than that at the sides. The rate of retrograde flow (Fig. 4H) at the center ('Center' in Fig. 4F) and side ('Side' in Fig. 4F) of the cell was inversely proportional to the rate of expansion (Fig. 4G), as seen in previous studies (Barnhart et al., 2011; Jurado et al., 2005; Vallotton et al., 2005).

Electroporation of keratocytes on an elastic substratum

If it is possible to load samples into cells on various types of substrata, the versatility of the new electroporator increases significantly. We tried to load Oregon Green dextran 10,000 MW into keratocytes on an elastic substratum that had been used for an experiment involving cyclic stretching of the substratum (Iwadate and Yumura, 2009; Iwadate et al., 2013). Electric field pulses were applied in the same manner as above. Fluorescence from Oregon

Green was detected in 208 of 253 cells (total from three experiments) that had been subjected to the electric pulses. Fig. 5A,B shows a DIC image and a fluorescence image of typical keratocytes, 5 min after application of the electric pulses. Fluorescence of Oregon Green was detected in all cells, although the cell indicated by an arrow in Fig. 5A was rounded by the shock of the pulses. The other cells actively migrated.

Electroporation of HL-60 cells and *Dictyostelium* cells using the new electroporator

In conventional electroporation, the electroporation conditions, e.g. the composition of the electroporation medium and the electric pulse conditions, affects its efficiency. The optimal condition is different in different cell types. We tested whether Oregon Green dextran 10,000 MW can be loaded into HL-60 and *Dictyostelium* cells using the new electroporator. Electric field pulses were applied to the medium between the electrodes twice at an interval of 20 s. The amplitude and the duration of the pulses were $400\,V\,cm^{-1}$ and 30 ms for HL-60 cells, and $300\,V\,cm^{-1}$ and 30 ms for *Dictyostelium* cells, respectively. Fluorescence from Oregon Green was detected in 147 of 197 cells (total from three experiments) for HL-60 cells and 187 of 209 cells (total from three experiments) for *Dictyostelium* cells that had been subjected to the electric pulses. Fig. 5C–F shows a DIC image and a fluorescence image of typical HL-60 cells (Fig. 5C,D) and *Dictyostelium* cells (Fig. 5E,F), 5 min after application of the electric pulses. Both cells actively migrated, indicating that our new electroporator can be used for various cell types.

DISCUSSION

We have developed a new electroporator that can be set on a microscope stage and requires very small samples. The efficiency of electroporation with our new device (Fig. 3D) is comparable to that of a normal volume electroporator that requires the adherent cells to be removed from the substratum (Usaj et al., 2010; Yumura et al., 1995).

Fluorochrome-conjugated phalloidin is used for staining of actin filaments (F-actin) in both fixed and live cells (Barnhart et al., 2011; Ofer et al., 2011; Okeyo et al., 2009a; Okeyo et al., 2009b). To visualize stress fibers in live keratocytes, we loaded Alexa phalloidin into the cells using the new electroporator. Several stress fibers were aligned perpendicular to the migrating direction in the cell body, as seen in previous studies (Miyoshi and Adachi, 2012; Okeyo et al., 2009a; Svitkina et al., 1997), indicating that loading Alexa phalloidin with the new device can be used to visualize F-actin in live cells without causing physiological damage.

The current consensus is that actin polymerization takes place at the leading edge of the lamellipodium during crawling cell migration (Iwadate and Yumura, 2008; Svitkina et al., 1997; Wang, 1985). The force generated by this actin polymerization induces expansion of the leading edge and retrograde flow of the polymerized F-actin. Fluorescence speckle microscopy (Jurado et al., 2005; Okeyo et al., 2009b; Schaub et al., 2007; Watanabe and Mitchison, 2002; Waterman-Storer and Salmon, 1997; Yam et al., 2007) is one of the most successful methods of estimating the rate of retrograde F-actin flow. Using our new electroporator, it was a simple matter to dilute the concentration of Alexa phalloidin in the electroporation medium from 100 to $25\,\mu mol\,l^{-1}$ to observe speckle staining of F-actin (Fig. 4C–H), indicating that the intracellular concentration of the probe can be easily regulated by changing its concentration in the electroporation medium.

Using our electroporator, Oregon Green could be loaded into keratocytes adhered not only to coverslips but also to an elastic silicone substratum without causing physiological damage (Fig. 5A,B). This suggests that the new device may allow electroporation for cells on various types of substrate, such as microstructured surface (Nikkhah et al., 2012), nanofibrous substrate (Tutak et al., 2013) and gels with different stiffness (Kawano and Kidoaki, 2011).

Oregon Green could be loaded into not only keratocytes but also HL-60 and *Dictyostelium* cells (Fig. 5). Optimal values of the electric field for each cell type are limited in a narrow range from 300 to $400\,V\,cm^{-1}$. This may be due to the use of electroporation medium with the same composition: Oregon Green with GFR. It is well known that the optimal amplitude and duration of the electric pulse in electroporation is strongly dependent on the composition of the electroporation medium. The narrow range of the electric field will be very useful for users, enabling them to adjust it for their particular cell types.

The application of electric pulses using our new electroporator did not cause keratocytes to peel off from the substratum (compare Fig. 3A and 3B). These results suggest that the new device is potentially useful not only for migrating cells but also for other non-migrating adherent cells, as the adhesive force of non-migrating cells is greater than that of keratocytes.

Using the new device, samples can be loaded into adherent cells on the stage of an inverted microscope while continuing to observe them. Thus, the new device has considerable promise as a tool for studying cells with limited numbers, such as primary cells, explanted directly from the donor organism, and particularly for examining small colonies of differentiated cells derived from induced pluripotent stem (iPS) cells. Because it is operated by connection to a commercially available auto-pipette, the new device is applicable for general rather than specialized use.

AUTHOR CONTRIBUTIONS

Y.I. invented the concept of the new electroporator. H.T. designed and developed the device. H.T. and C.O. performed experiments and data analysis. T.M. and Y.I. prepared the manuscript prior to submission.

COMPETING INTERESTS

No competing interests declared.

REFERENCES

Barnhart, E. L., Lee, K.-C., Keren, K., Mogilner, A. and Theriot, J. A. (2011). An adhesion-dependent switch between mechanisms that determine motile cell shape. *PLoS Biol.* **9**, e1001059.

Boitano, S., Dirksen, E. R. and Sanderson, M. J. (1992). Intercellular propagation of calcium waves mediated by inositol trisphosphate. *Science* **258**, 292-295.

Chang, D. C. and Reese, T. S. (1990). Changes in membrane structure induced by electroporation as revealed by rapid-freezing electron microscopy. *Biophys. J.* **58**, 1-12.

Grimm, H. P., Verkhovsky, A. B., Mogilner, A. and Meister, J.-J. (2003). Analysis of actin dynamics at the leading edge of crawling cells: implications for the shape of keratocyte lamellipodia. *Eur. Biophys. J.* **32**, 563-577.

Iwadate, Y. and Yumura, S. (2008). Actin-based propulsive forces and myosin-II-based contractile forces in migrating *Dictyostelium* cells. *J. Cell Sci.* **121**, 1314-1324.

Iwadate, Y. and Yumura, S. (2009). Cyclic stretch of the substratum using a shape-memory alloy induces directional migration in *Dictyostelium* cells. *Biotechniques* **47**, 757-767.

Iwadate, Y., Okimura, C., Sato, K., Nakashima, Y., Tsujioka, M. and Minami, K. (2013). Myosin-II-mediated directional migration of dictyostelium cells in response to cyclic stretching of substratum. *Biophys. J.* **104**, 748-758.

Jurado, C., Haserick, J. R. and Lee, J. (2005). Slipping or gripping? Fluorescent speckle microscopy in fish keratocytes reveals two different mechanisms for generating a retrograde flow of actin. *Mol. Biol. Cell* **16**, 507-518.

Kawano, T. and Kidoaki, S. (2011). Elasticity boundary conditions required for cell mechanotaxis on microelastically-patterned gels. *Biomaterials* **32**, 2725-2733.

Kinosita, K., Jr and Tsong, T. Y. (1977). Formation and resealing of pores of controlled sizes in human erythrocyte membrane. *Nature* **268**, 438-441.

Lee, J., Ishihara, A., Theriot, J. A. and Jacobson, K. (1993). Principles of locomotion for simple-shaped cells. *Nature* **362**, 167-171.

Miyoshi, H. and Adachi, T. (2012). Spatiotemporal coordinated hierarchical properties of cellular protrusion revealed by multiscale analysis. *Integr Biol (Camb)* **4**, 875-888.

Mizuno, T. and Sekiguchi, Y. (2011). Staurosporine induces lamellipodial widening in locomoting fish keratocytes by abolishing the gradient from radial extension of leading edge. *Biophysics (Oxf.)* **7**, 69-75.

Mizuno, T., Kagami, O., Sakai, T. and Kawasaki, K. (1996). Locomotion of neutrophil fragments occurs by graded radial extension. *Cell Motil. Cytoskeleton* **35**, 289-297.

Mizuno, T., Sakai, T., Yoshioka, K. and Kawasaki, K. (2003). Difference-from-prediction imaging for high resolution shape analysis of locomoting cells. *bioimages* **11**, 61-66.

Mogilner, A. and Keren, K. (2009). The shape of motile cells. *Curr. Biol.* **19**, R762-R771.

Nikkhah, M., Edalat, F., Manoucheri, S. and Khademhosseini, A. (2012). Engineering microscale topographies to control the cell-substrate interface. *Biomaterials* **33**, 5230-5246.

Ofer, N., Mogilner, A. and Keren, K. (2011). Actin disassembly clock determines shape and speed of lamellipodial fragments. *Proc. Natl. Acad. Sci. USA* **108**, 20394-20399.

Okeyo, K. O., Adachi, T., Sunaga, J. and Hojo, M. (2009a). Actomyosin contractility spatiotemporally regulates actin network dynamics in migrating cells. *J. Biomech.* **42**, 2540-2548.

Okeyo, K. O., Adachi, T. and Hojo, M. (2009b). Dynamic coupling between actin network flow and turnover revealed by flow mapping in the lamella of crawling fragments. *Biochem. Biophys. Res. Commun.* **390**, 797-802.

Raptis, L., Vultur, A., Brownell, H. L., Tomai, E., Anagnostopoulou, A., Arulanandam, R., Cao, J. and Firth, K. L. (2008). Electroporation of adherent cells in situ for the study of signal transduction and gap junctional communication. *Methods Mol. Biol.* **423**, 173-189.

Schaub, S., Bohnet, S., Laurent, V. M., Meister, J.-J. and Verkhovsky, A. B. (2007). Comparative maps of motion and assembly of filamentous actin and myosin II in migrating cells. *Mol. Biol. Cell* **18**, 3723-3732.

Svitkina, T. M., Verkhovsky, A. B., McQuade, K. M. and Borisy, G. G. (1997). Analysis of the actin-myosin II system in fish epidermal keratocytes: mechanism of cell body translocation. *J. Cell Biol.* **139**, 397-415.

Teruel, M. N. and Meyer, T. (1997). Electroporation-induced formation of individual calcium entry sites in the cell body and processes of adherent cells. *Biophys. J.* **73**, 1785-1796.

Tutak, W., Sarkar, S., Lin-Gibson, S., Farooque, T. M., Jyotsnendu, G., Wang, D., Kohn, J., Bolikal, D. and Simon, C. G., Jr (2013). The support of bone marrow stromal cell differentiation by airbrushed nanofiber scaffolds. *Biomaterials* **34**, 2389-2398.

Usaj, M., Trontelj, K., Miklavcic, D. and Kanduser, M. (2010). Cell-cell electrofusion: optimization of electric field amplitude and hypotonic treatment for mouse melanoma (B16-F1) and Chinese Hamster ovary (CHO) cells. *J. Membr. Biol.* **236**, 107-116.

Vallotton, P., Danuser, G., Bohnet, S., Meister, J.-J. and Verkhovsky, A. B. (2005). Tracking retrograde flow in keratocytes: news from the front. *Mol. Biol. Cell* **16**, 1223-1231.

Wang, Y. L. (1985). Exchange of actin subunits at the leading edge of living fibroblasts: possible role of treadmilling. *J. Cell Biol.* **101**, 597-602.

Watanabe, N. and Mitchison, T. J. (2002). Single-molecule speckle analysis of actin filament turnover in lamellipodia. *Science* **295**, 1083-1086.

Waterman-Storer, C. M. and Salmon, E. D. (1997). Actomyosin-based retrograde flow of microtubules in the lamella of migrating epithelial cells influences microtubule dynamic instability and turnover and is associated with microtubule breakage and treadmilling. *J. Cell Biol.* **139**, 417-434.

Yam, P. T., Wilson, C. A., Ji, L., Hebert, B., Barnhart, E. L., Dye, N. A., Wiseman, P. W., Danuser, G. and Theriot, J. A. (2007). Actin-myosin network reorganization breaks symmetry at the cell rear to spontaneously initiate polarized cell motility. *J. Cell Biol.* **178**, 1207-1221.

Yang, T. A., Heiser, W. C. and Sedivy, J. M. (1995). Efficient in situ electroporation of mammalian cells grown on microporous membranes. *Nucleic Acids Res.* **23**, 2803-2810.

Yumura, S., Matsuzaki, R. and Kitanishi-Yumura, T. (1995). Introduction of macromolecules into living *Dictyostelium* cells by electroporation. *Cell Struct. Funct.* **20**, 185-190.

Zheng, Q. A. and Chang, D. C. (1991). High-efficiency gene transfection by in situ electroporation of cultured cells. *Biochim. Biophys. Acta* **1088**, 104-110.

Zimmermann, U., Pilwat, G., Holzapfel, C. and Rosenheck, K. (1976). Electrical hemolysis of human and bovine red blood cells. *J. Membr. Biol.* **30**, 135-152.